Available online at www.sciencedirect.com
SCIENCE DIRECT®
Journal of Solid State Chemistry 177 (2004) 3721–3728
JOURNAL OF SOLID STATE CHEMISTRY
www.elsevier.com/locate/jssc

Mu-28: an open-framework fluorogallophosphate with a three-dimensional 12-membered ring channel system

Ludovic Josien[a], Angélique Simon-Masseron[a,*], Volker Gramlich[b], Florence Porcher[c], Joël Patarin[a]

[a]Laboratoire de Matériaux Minéraux CNRS UMR 7016, Université de Haute-Alsace, 3, rue Alfred Werner, F-68093 Mulhouse Cedex, France
[b]Laboratorium für Kristallographie, ETH-Zentrum, Sonneggstrasse 5, CH-8092 Zürich, Switzerland
[c]Laboratoire de Cristallographie et Modélisation des Matériaux Minéraux et Biologiques CNRS UMR 7036, Faculté des sciences, Université Henri Poincaré Nancy 1, B.P. 239, 54506 Vandoeuvre-Lès-Nancy Cedex, France

Received 16 March 2004; received in revised form 22 June 2004; accepted 22 June 2004
Available online 23 August 2004

Abstract

A new three-dimensional (3-D) microporous fluorogallophosphate, named Mu-28, was obtained by hydrothermal synthesis. It was obtained in the presence of fluoride ions with 1,4-dimethylpiperazine as organic template. This new fluorogallophosphate, with chemical formula $[Ga_{20}P_{20}O_{80}(OH)_6F_6(H_2O)_4(C_6H_{16}N_2)_6]$ $8H_2O$, crystallizes in the monoclinic system space group $P2_1$ with the following unit cell parameters: $a = 13.23(1)$ Å, $b = 15.40(1)$ Å, $c = 14.80(1)$ Å, $\beta = 95.10(9)^\circ$ ($Z = 1$, $R_1 = 0.0435$ [$I > 2\sigma(I)$]). Its structure was determined by single-crystal X-ray diffraction with the help of ^{31}P NMR spectroscopy. Mu-28 consists of a complex arrangement of $GaO_3(OH,F)(H_2O)_2$, $GaO_4(OH)F$ and $GaO_4(OH)_2$ octahedra, GaO_4F trigonal bipyramids and $GaO_3(OH,F)$ and PO_4 tetrahedra. It displays a 3-D channel system delimited by 12-membered ring openings.

Keywords: 1,4-dimethylpiperazine; Fluoride; Fluorogallophosphate; Single crystal structure elucidation

1. Introduction

Six-ring substituted amines as structure directing agent have been widely used in the synthesis of microporous materials. It seems that those molecules lead to large pore openings structures. For example, in the phosphates family, the fluorogallophosphate ULM-16 with 16-membered ring openings (16 MR) [1] and the zincophosphate ND-1 (24 MR) [2] were obtained in the presence of cyclohexylamine and 1,2-diaminocyclohexane, respectively.

Surprisingly, few derivatives of the piperazine have been used for the synthesis of gallophosphates (piperazine itself [3–7], DABCO (diazabicyclo[2,2,2] octane) [8–13], R-2-methylpiperazine [14] and 1,4-bis(aminopropyl)piperazine [15]). More recently, in our laboratory, a systematic study of *N*-substituted piperazine derivatives has been undertaken. A large number of known and unknown phases were obtained with or without fluoride ions in the starting mixture [16–18].

Among these materials, the synthesis and the crystal structure determination of a new layered fluorogallophosphate named Mu-23 was reported [17]. It was prepared in the presence of 1,4−dimethylpiperazine as organic template. Mu-23 was obtained as pure phase but in some cases, it co-crystallized with an unknown product named phase INC in Ref. [17]. In this paper, the synthesis and the crystal structure determination by X-ray diffraction of this latter phase renamed Mu-28 are described. The characterization of this new 3-D fluorogallophosphate by solid state NMR spectroscopy is also reported.

*Corresponding author. Fax: +33-3-89-33-68-85.
E-mail address: a.simon@univ-mulhouse.fr (A. Simon-Masseron).

0022-4596/$ - see front matter © 2004 Elsevier Inc. All rights reserved.
doi:10.1016/j.jssc.2004.06.041

2. Experimental section

2.1. Synthesis

The following reactants were used to prepare the synthesis mixture: the gallium source was an amorphous gallium oxyhydroxide (GaOOH) that was prepared by heating a gallium nitrate aqueous solution (Rhône-Poulenc) at 250 °C for 24 h. The others reactants were ortho-phosphoric acid (Labosi 85%), hydrofluoric acid (Carlo Erba 40%) and 1,4-dimethylpiperazine (DMPIP) (Aldrich 98%). The batch molar composition is 1:1:2:160:2; Ga_2O_3:P_2O_5:HF:H_2O:DMPIP. The mixture was prepared by adding under stirring the phosphoric acid (0.58 g, 5 mmol) to a suspension of GaOOH (0.51 g, 5 mmol) in desionized water (6.98 g, 388 mmol). Homogenization times of 10 min are applied before the successive additions of hydrofluoric acid (0.25 g, 5 mmol) and amine (0.57 g, 5 mmol). Then, the mixture was aged under stirring for 1 h at room temperature and transferred to a 40 mL PTFE lined stainless steel autoclave. The crystallization was carried out under static conditions at 130 °C during 6 days. The starting and final pH of the mixture were equal to 5. After heating, the product was recovered, washed with desionized water and dried at 60 °C overnight.

2.2. Characterization techniques

The morphology and size of the crystals were determined by scanning electron microscopy using a Philips XL30 microscope.

The powder XRD patterns were obtained with Cu$K\alpha_1$ radiation on a STOE STADI-P diffractometer equipped with a curved germanium (111) primary monochromator and a linear position sensitive detector. High-temperature X-ray diffraction was performed using a variable temperature photographic chamber (Huber, model 631) attached to the same X-ray generator (Cu$K\alpha_1$ radiation) in which the sample was kept in a flow of dry air.

Single crystal X-ray diffraction was carried out with Cu$K\alpha$ radiation in omega scan mode on a Picker 4-circle STOE diffractometer equipped with a graphite monochromator.

The Ga and P analyses were performed by inductively coupled plasma emission spectroscopy. After mineralization of the as-synthesized sample, fluorine was determined using a fluoride ion-selective electrode. The amounts of carbon and nitrogen were determined by coulometric and catharometric methods, respectively after calcination of the sample.

Thermogravimetric (TGA) and differential thermal analyses (DTA) were performed under air on a Setaram Labsys thermoanalyser with a heating rate of 5 °C min^{-1} until 850 °C. At this final temperature, a gray residue is obtained. Calcination at 1000 °C is necessary to obtain a white product and therefore the total amount of the organic template.

The ^{13}C CP MAS NMR spectrum was recorded on a Bruker MSL 300 spectrometer and ^{31}P and ^{19}F NMR spectra on a Bruker DSX 400 spectrometer. The recording conditions of the CP MAS and MAS spectra are reported in supporting information.

3. Results and discussion

3.1. Synthesis and crystal morphology

The most representative syntheses leading to the formation of the fluorogallophosphate Mu-28 are given in Table 1. Large crystals of Mu-28 can be obtained when the crystallization temperature is high (see sample A). However, the presence of small peaks corresponding to an impurity on the XRD pattern (not shown) at 10.24° and 10.98° 2θ prompts us to optimize the synthesis conditions. It was finally possible to prepare a pure Mu-28 sample when a low temperature was applied (130 °C instead of 180 °C, sample B, Table 1). But the crystal size was smaller even with a longer crystallization time. On the other hand, the decrease in the gallium amount (samples C and D, Table 1) leads to the formation of the previously described layered material Mu-23.

Pure Mu-28 samples consist of large white spheres of aggregated crystals (spheres diameter up to 1 mm). Individual crystals seem to display a prismatic morphology and their sizes range from $50 \times 50 \times 100$ to $100 \times 200 \times 400\,\mu m^3$.

3.2. Structure determination

The powder XRD pattern of Mu-28 (Fig. 1a) was first indexed in the monoclinic symmetry with the following unit cell parameters: $a = 13.229(16)$ Å, $b = 15.396(12)$ Å, $c = 14.800(15)$ Å, $\beta = 95.10(9)°$. The space group $P2_1/n$ was in agreement with the extinction rules obtained from Weissenberg films.

Table 1
Summary of syntheses performed in the system x Ga_2O_3–1 P_2O_5–2 HF–160 H_2O–2 DMPIP

Sample	Ga_2O_3 (x)	Temperature (°C)	Crystallization time (days)	Products (XRD)
A	1	180	1.5	Mu-28[a] + non-identified phase
B	1	130	6	Mu-28
C	0.5	130	6	Mu-23 + Mu-28[a]
D	0.25	130	6	Mu-23

[a]Major phase.

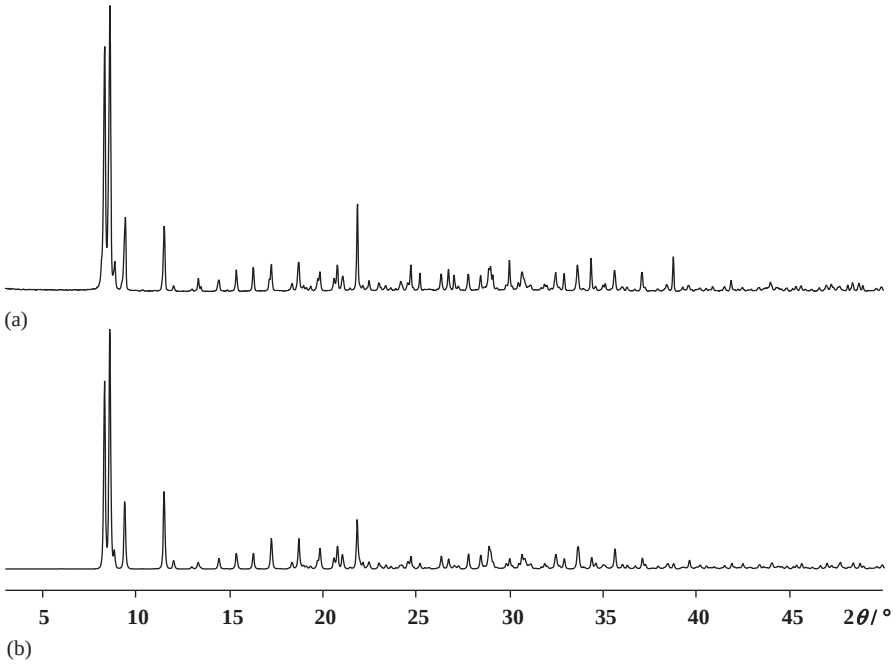

Fig. 1. (a) Experimental XRD pattern of Mu-28, (b) simulated XRD pattern of Mu-28 calculated from the single crystal structure data.

For the structure determination, a single crystal with dimensions $40 \times 50 \times 100\,\mu m^3$ was selected. Three thousand two hundred and thirty seven independent reflections were recorded from 3.00° to 50.00°θ for which 2060 fulfilled the condition $I > 2\sigma(I)$. The structure was first refined with the space group $P2_1/n$. The resulting R value (R_1obs) was about 12%. This high value comes from an extremely pronounced pseudosymmetry. The distortion of one amine molecule and the splitting of the Ga(1) atoms into one octahedra $Ga(1)O_5X$ (X = OH or F) and one tetrahedra $Ga(1')O_3X$ (see description) are responsible of the deviation from the centrosymmetric to non-centrosymmetric space group $P2_1$. Due to this extremely pronounced pseudosymmetry, the n-glide extinctions are nearly perfectly fulfilled.

Beside of the high final reliability factors ($R_1 = 0.12$ ($R_1 = \Sigma||F_0|-|F_c||/\Sigma|F_0|$); w$R_2 = 0.32$ ($R_2 = \{\Sigma w(F_0^2-F_c^2)^2/\Sigma w(F_0^2)^2\}^{1/2}$)) with $P2_1/n$ space group, the most important disagreement comes from ^{31}P solid state NMR spectroscopy. Indeed the NMR spectrum (see below) shows unambiguously the presence of 10 crystallographic non-equivalent P sites whereas with the space group $P2_1/n$, only five distinct crystallographic phosphorus sites are expected. According to the extinction rules, $P2_1$ seems to be the best candidate. The other monoclinic space groups ($P2$, Pm, Pc), with a multiplicity of 2 do not fit well. A second refinement with the non-centrosymmetric space group $P2_1$, allowed us to place all framework atoms, the amine molecules (1,4-dimethylpiperazine) and water molecules. The reliability factors finally converged to $R_1 = 0.04$; w$R_2 = 0.10$ for $I > 2\sigma(I)$. A summary of the experimental and crystallographic data is reported in Table 2.

From direct methods using SHELXS-86 [19] the positions of gallium and phosphorus atoms were revealed. All the remaining atoms, except the hydrogen ones, were located from successive Fourier maps using SHELXL-93 [20]. Hydrogen atoms of amine molecules were placed with geometrical constraints. Non-hydrogen atoms were refined with anisotropic displacement parameters. The resulting atomic coordinates including the equivalent isotropic displacement parameters and the selected bond lengths and angles are reported in supplementary information. As a comparison with experimental data, the simulated XRD pattern of Mu-28 calculated from structure data is given in Fig. 1b.

According to the elemental analyses, the as-synthesized Mu-28 sample has the following composition (wt%): Ga 32.6, P 13.6, F 2.6, N 3.7, C 9.7. The results of these analyses are in good agreement with the theoretical composition obtained from the unit cell formula $[Ga_{20}P_{20}O_{80}(OH)_6F_6(H_2O)_4(C_6H_{16}N_2)_6]\cdot 8H_2O$ found by structure determination: Ga 31.5, P 14.0, F 2.6, N 3.8, C 9.8.

The thermal behavior of Mu-28 was investigated by high-temperature XRD analysis and TG/DTA thermal analyses. The TG and DTA curves of Mu-28 are given in Fig. 2. The DTA curve presents two endothermic peaks at 100 °C and 150 °C. These peaks could be associated on the TG curve to a weight loss of 4.8% between 60 °C and 200 °C that is attributed to the removal of structural water and water coordinated to

Table 2
Summary of the experimental and crystallographic data of the fluorogallophosphate Mu-28

Unit cell chemical formula		$[Ga_{20}P_{20}O_{80}(OH)_6F_6(H_2O)_4(C_6H_{16}N_2)_6]\cdot 8H_2O$	
Crystal system and space group		Monoclinic; $P2_1$	
Formula weight ($g\,mol^{-1}$)		4423.26	
a (Å)	α (deg)	13.23(1)	90
b (Å)	β (deg)	15.40(1)	95.10(9)
c (Å)	γ (deg)	14.80(1)	90
V (Å^3)		3002(5)	
Crystal size (μm)		$40 \times 50 \times 100$	
Diffractometer		Picker STOE 4-circles	
Radiation source and wavelength (Å)		Cu$K\alpha$ 1.54178	
Absorption coefficient (mm^{-1})		8.645	
F(000)		2185	
Data collection temperature (K)		293(2)	
θ range (deg)		3.00–50.00	
Index ranges		$-14<h<14, -1<k<16, -1<l<15$	
Independent reflections		3237	
Observed reflections [$I>2\sigma(I)$]		2060	
Data/restraints/parameters		3237/61/485	
Residuals (observed data) [$I>2\sigma(I)$]		$R_1 = 0.0435$, w$R_2 = 0.1017$	
Residuals (all data)		$R_1 = 0.0795$, w$R_2 = 0.1275$	
Largest diff. peak and hole (e/Å^3)		0.835 and −0.605	

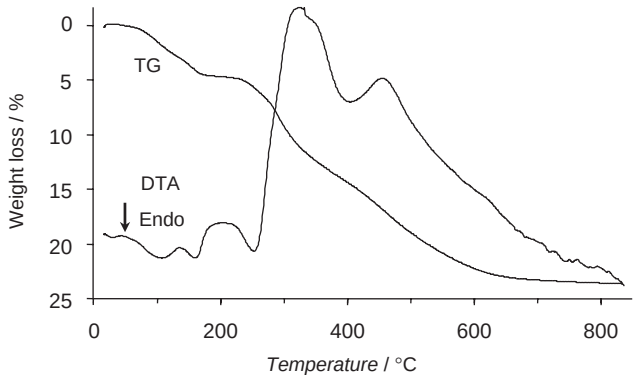

Fig. 2. Thermal analyses (TG, DTA) under air of the fluorogallophosphate Mu-28.

Ga(1) (see below). Another endothermic peak is observed at 250 °C just before the exothermic peaks of the organic template oxidation. It could be assigned to the removal of water arising from dehydroxylation reactions (presence of terminal Ga–OH and P–OH groups), or/and to the removal of hydrofluoric acid. However, around 300 °C, several phenomena occurs and it is difficult to assign specifically a weight loss to one reaction. Nevertheless, between 250 °C and 850 °C, a global weight loss of 19% can be measured. From high-temperature XRD analyses, the structure collapses at 260 °C. After heating at 850 °C, the color of the remaining solid is still black which indicates the presence of traces of organic residues. Their removal only occurs at 1000 °C (1.2 wt%) and then the resulting white material corresponds to a cristobalite-type gallophosphate. Therefore, the total weight loss observed between 10 °C and 1000 °C is close to 25 wt% which is in good agreement with the amounts of water, template and fluorine determined by crystal structure determination and chemical analyses (24.5 wt%).

3.3. Structure description

Mu-28 has a complex 3-D framework built from $GaO_3(OH,F)(H_2O)_2$, $GaO_4(OH)F$ and $GaO_4(OH)_2$ octahedra, GaO_4F trigonal bipyramid, $GaO_3(OH,F)$ and PO_4 tetrahedra. The asymmetric unit of Mu-28 contains 10 crystallographically non-equivalent P and Ga atoms, respectively.

The structure is built from 4-, 6-, 12-membered rings (MR) and an interesting secondary building unit (SBU) composed of 8T atoms (T=Ga, P) and two oxygen atoms coordinated to three gallium atoms (Fig. 3). This SBU is pentacyclic and has been previously described in some metal phosphate materials [21–37] (Table 3). The different connecting scheme of pentacyclic units in all these materials is shown in Fig. 4. In most of them and without relation with the M/P molar ratio, two successive units are corner sharing (connections types 1 and 2 in Table 3 and Fig. 4). Only the structure of the gallophosphate $[Ga_4(HPO_4)_2(PO_4)_3(OH)_2F(C_4N_2H_{14})_2]\cdot 6H_2O$ [37] links its units by $PO_3(OH)$ bridges (Fig. 4, connection type 3). The fluorogallophosphate Mu-28 exhibits an original connection type: its pentacyclic units are connected by a four ring (Fig. 4, connection type 4).

As previously observed for other metallophosphates with the pentacyclic unit, the three coordinated oxygen atoms (O(18) and O(18′)) in Mu-28 structure (see Fig. 3)

are in fact hydroxyl groups. They are bonded to Ga(5), Ga(5′) and Ga(4) or Ga(4′) and compared to usual Ga–O bond lengths, long Ga–O distances ($2.05(2)\,\text{Å} < d(\text{Ga–O}) < 2.14(2)\,\text{Å}$) are observed. Other three-coordinated atoms were attributed to bridging fluorine atoms F(2) and F(2′). These atoms are also in interaction with three Ga atoms (Ga(2), Ga(3), Ga(4) and Ga(2′), Ga(3′), Ga(4′), respectively) but unlike the previous oxygen atoms, both fluorine atoms display one weak bond ($d(\text{Ga}(3')-\text{F}(2')) = 2.77(3)\,\text{Å}$; $d(\text{Ga}(2)-\text{F}(2)) = 2.47(2)\,\text{Å}$) and two stronger bonds ($2.02(1) < \text{d(Ga}-\text{F}(2)$ or $\text{Ga–F}(2')) < 2.29(2)\,\text{Å}$). Such bond lengths are longer than those previously found in other fluorogallophosphates (typically $1.94 < d(\text{Ga}-\text{F}) < 2.04\,\text{Å}$ [38–39]) but the presence of the third weak interaction could explain the gap to ideal distances.

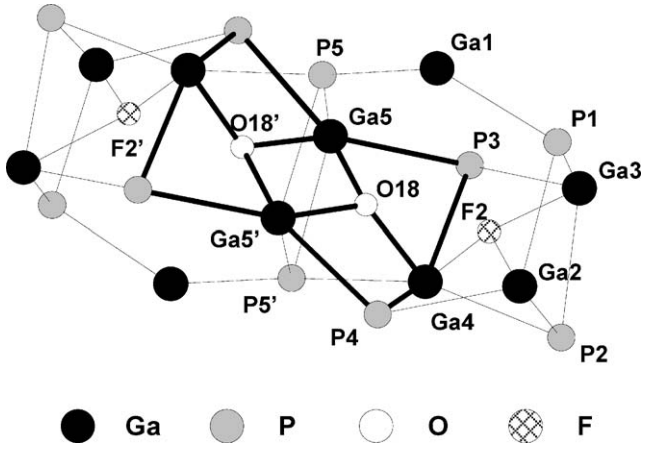

Fig. 3. View of the G unit showing the pentacyclic unit. For clarity, the bonds of the latter have been thicken.

Mu-28 structure can also be described as an arrangement of $[4^6 6^2]$ cages (afterwards called G unit) (Fig. 3) and 4-membered rings (Fig. 5). The connection of those G units via 4-MR in the three space directions leads to the 3-D structure which displays a 3-D channel system delimited by 12-MR openings (Fig. 6). Four water molecules and three biprotonated 1,4-dimethylpiperazine are occluded in this channel system. These molecules are in hydrogen interaction with the framework atoms, especially with terminal groups $X(1)$ and $X(1')$ or terminal oxygen atoms O(7) and O(7′).

As previously seen in the structure determination section, the non-centrosymmetry of the structure is due to the non-equivalence of Ga(1) and Ga(1′) sites in the 4-MR unit connecting the G units (Fig. 5). Indeed, the environment of these two Ga atoms differs by the presence of various terminal groups. The attribution of these groups was established on the basis of chemical and thermal analyses, ^{19}F MAS NMR spectroscopy and bond-valence calculations [40]. The two long Ga(1)–O distances ($d = 2.139(14)\,\text{Å}$ and $d = 2.10(2)\,\text{Å}$) were attributed to the presence of water molecules O(5W) and O(6W), respectively. Short distances Ga(1)–$X(1)$ ($d = 1.86(1)\,\text{Å}$) and Ga(1′)–$X(1')$ ($d = 1.80(2)\,\text{Å}$) correspond to the presence of a 50/50 statistic repartition of hydroxyl groups and fluorine atoms over the two positions. This repartition could justify the low charge found with the bond valence calculation when $X(1)$ and $X(1')$ are constrained to be only hydroxyl groups (Table 4). This hypothesis is also in agreement with the ^{19}F MAS NMR spectra (see below).

Phosphorus atoms P(1), P(3) and P(4) exhibit an average P–O distance of ca. 1.52 Å and share all their oxygen atoms with gallium atoms. As previously observed for other gallophosphates [41], the short

Table 3
Phosphate based material containing the pentacyclic unit

Name (reference)	Structure directing agent	Chemical formula	Connection type	M/P (molar ratio)
Leuco-phosphite [21]	K	$[Fe_4(OH)_2(H_2O)_2(PO_4)_4K_2]\cdot 2H_2O$	(1)	1
[22][a,b]	/	$[GaPO_4]_2\cdot 4H_2O$	(1)	1
$GaPO_4$-15[b] [23]	NH_4	$[Ga_2(PO_4)_2(OH)(H_2O)(NH_4)]\cdot H_2O$	(1)	1
[24][a,b]	Rb	$[Ga_2(PO_4)_2(OH)(H_2O)Rb]\cdot H_2O$	(1)	1
[25][a,b]	Na	$[Ga_2(PO_4)_2(OH)Na]$	(1)	1
$AlPO_4$-15[b] [26]	NH_4	$[Al_2(PO_4)_2(OH)(H_2O)(NH_4)]\cdot H_2O$	(1)	1
[27-29][a,b]	NH_4; Rb; Cs	$[Mo_2P_2O_{10}(NH_4)]\cdot H_2O$	(1)	1
[30][a,b]	NH_4	$[V_2(OH)(PO_4)_2(H_2O)(NH_4)]\cdot H_2O$	(1)	1
[30][a]	Rb	$[(Mo_9V_3O_6)(PO_4)_{10}(HPO_4)_3(OH)_9Rb]\cdot 8H_2O$	(1)	0.92
UiO-13 [31]	Ethylenediamine	$[Al_2P_2O_9(C_2N_2H_{10})]$	(1)	1
UiO-26 [32]	1,3-diaminopropane	$[Al_4O(PO_4)_4(H_2O)(C_3N_2H_{12})]$	(1)	1
$GaPO_4$-12 [33]	Ethylenediamine	$[Ga_3(PO_4)_3(C_2N_2H_8)]\cdot H_2O$	(1)	1
[34,35][a]	1,3-diaminopropane	$[Fe_4(HPO_4)_2(PO_4)_3(OH)_3(C_3N_2H_{12})_2]\cdot xH_2O$	(2)	0.8
ICL-1 [36]	1,4-diaminobutane	$[Ga_4(HPO_4)_2(PO_4)_3(OH)_2F(C_4N_2H_{14})_2]\cdot 6H_2O$	(2)	0.8
[37][a]	Ethylenediamine	$[Ga_{2.4}V_{1.6}(HPO_4)_5(PO_4)_3H(OH)_2(C_2N_2H_{10})_4]$	(3)	0.5
Mu-28	DMPIP	$[Ga_{20}P_{20}O_{80}(OH)_6F_6(H_2O)_4(C_6H_{16}N_2)_6]\cdot 8H_2O$	(4)	1

[a]No name attributed.
[b]Material isostructural to leucophosphite.

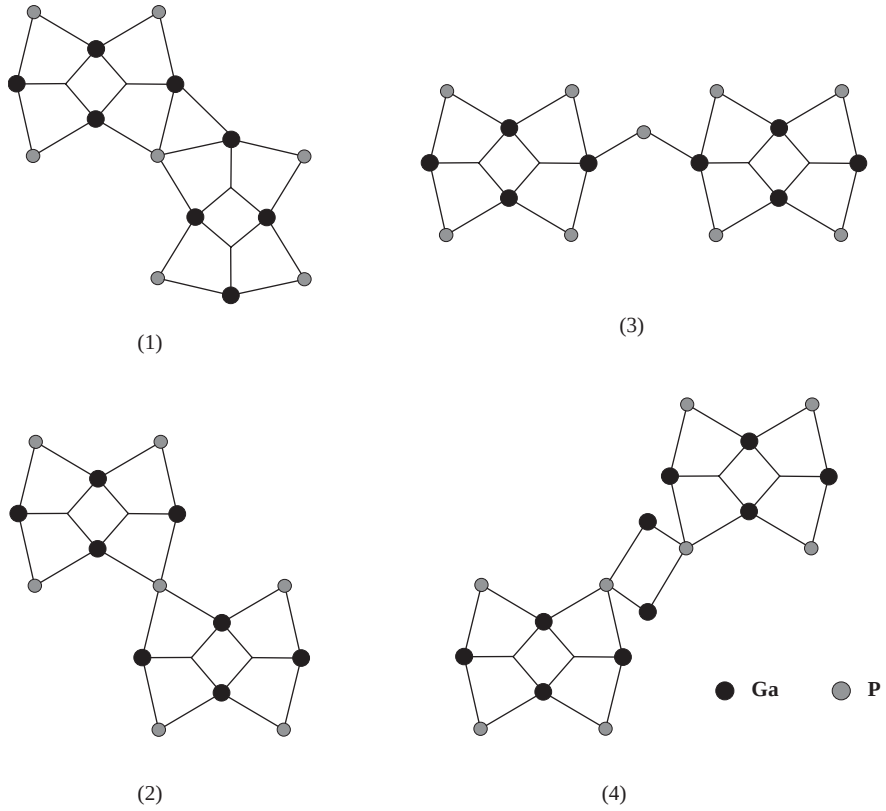

Fig. 4. Different connection types of pentacyclic units.

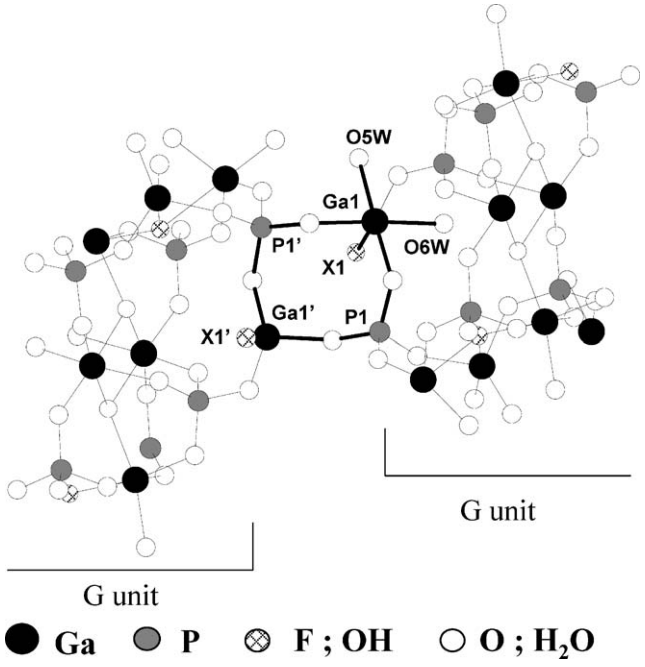

Fig. 5. Representation of the non-centrosymmetric four ring connecting two G units.

P(2)–O(7) and P(2′)–O(7′) distances of 1.49(2) Å reveal the presence of P=O groups; these phosphorus share only three of their oxygen atoms with Ga atoms.

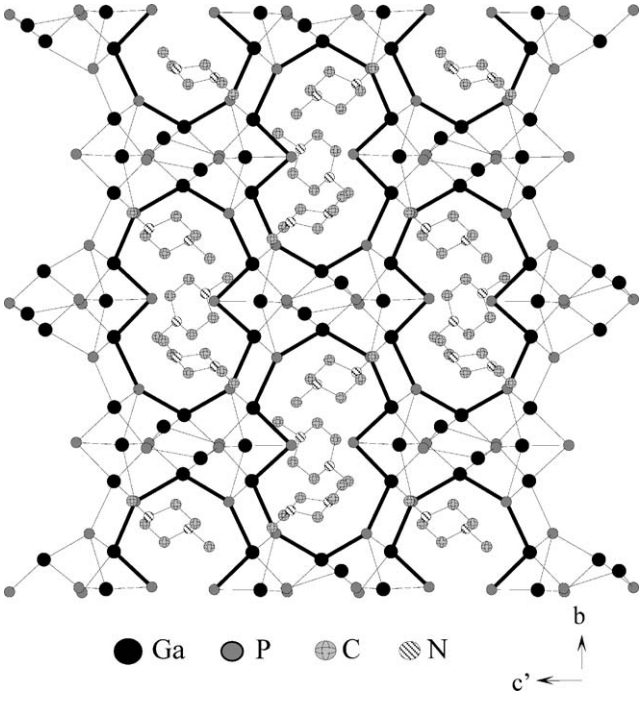

Fig. 6. View along [100] direction of Mu-28 structure showing the 12-MR openings of the channel system (thicker lines) and the three non-equivalent amines occluded in the channels. Water molecules, framework oxygen and fluorine atoms are omitted for clarity. $c' = c \times \cos(\beta - 90)$.

4. Solid-state NMR spectroscopy

4.1. ^{31}P NMR

The ^{31}P MAS NMR spectrum of the fluorogallophosphate Mu-28 displays six main signals at 3.1, −1.2, −2.7, −6.3, −9.5 and −12.7 ppm (Fig. 7). A decomposition of this highly resolved spectrum reveals in fact seven components with the following relative areas 1:1:2:1:3:1:1 showing therefore the presence of 10 non-equivalent phosphorus sites. From CP MAS NMR experiments performed at different contact times, an increase in the components located at −4.3 and −1.2 ppm was observed. The corresponding signals might be assign to P(2) and P(2′) sites which are in strong hydrogen interaction with water molecules (d(P(2) = O(7)...O(1W)) = 2.76(2) Å, d(P(2′) = O(7′)...O(2W)) = 2.68(5) Å).

4.2. ^{13}C NMR

The ^{13}C CP MAS spectrum (not shown) displays three signals at 52.1, 45.0 and 43.1 ppm. The broad peak at 52.1 ppm was assigned to the CH_2 groups. The two other signals at 45.0 and 43.1 ppm correspond to the methyl groups of the three non-equivalent amines.

Table 4
Bond-valence calculation according to Brown [40] for Ga(1) and Ga(1′) terminal groups

Atoms	H[a]	Ga(1)	Ga(1′)	Σs	Expected valence
O(5W)	2 × 0.8	0.33		1.93	2
O(6W)	2 × 0.8	0.37		1.97	2
X(1)[b]	0.8	0.71		1.51	2
X(1′)[b]	0.8		0.83	1.63	2

[a]On the basis of an O–H bond length of 0.96 Å
[b]In these calculations X(1) and X(1′) were constrained to be OH groups only.

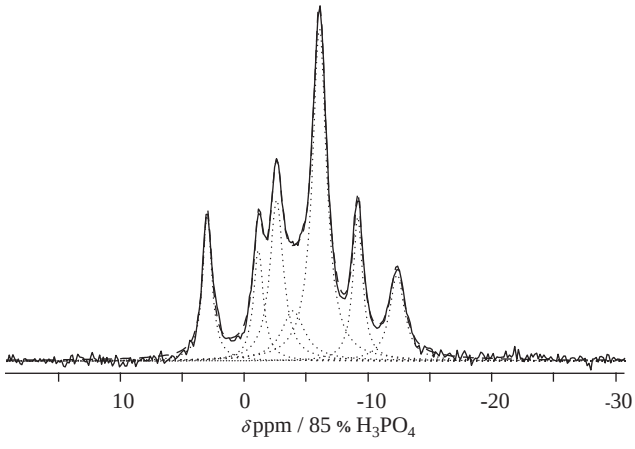

Fig. 7. ^{31}P MAS NMR spectrum (continuous line) and decomposition (dashed lines) of the fluorogallophosphate Mu-28 (*: spinning side bands).

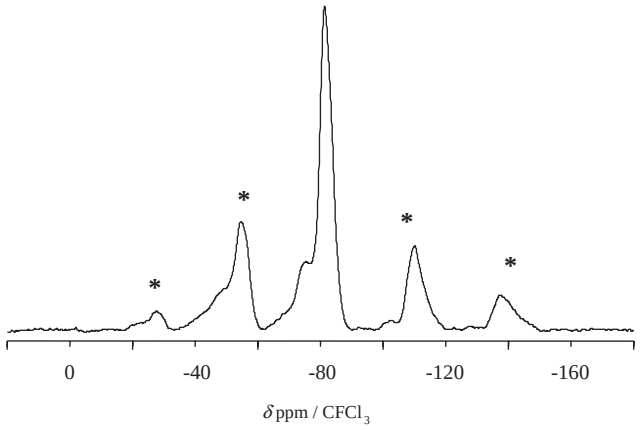

Fig. 8. ^{19}F MAS NMR spectrum of the fluorogallophosphate Mu-28 (*: spinning side bands).

4.3. ^{19}F NMR

The ^{19}F MAS NMR spectrum of the title compound is given in Fig. 8. Two resonances are observed at −78.8 and −82.3 ppm. The intensity ratio close to 1:5 is in agreement with the structure determination. Indeed the signal at −78.8 ppm can be attributed either to X(1) or X(1′) group, this position being half occupied by a fluorine atom and half occupied by an hydroxyl group. The signal at −82.3 ppm corresponds to the other fluorine atoms: F(2), F(2′) and X(1′) or X(1).

5. Conclusion

The use of 1,4-dimethylpiperazine as structure-directing agent in the system Ga_2O_3–P_2O_5–HF–H_2O leads to the crystallization of a new fluorogallophosphate: $[Ga_{20}P_{20}O_{80}(OH)_6F_6(H_2O)_4(C_6H_{16}N_2)_6]\cdot 8H_2O$, named Mu-28.

The structure of this new material consists on the interconnection of simple four ring and double [$4^6 6^2$] cages. Fluorine atoms and hydroxyl groups are occluded in these [$4^6 6^2$] cages. The arrangement of such building units leads to a 3-D channel system with 12-MR windows. Protonated amines and water molecules localized in the channel system are in strong hydrogen interactions with the terminal framework atoms.

Acknowledgment

The authors thank "Institut Français du Pétrole" (IFP) which kindly provided the gallium nitrate source.

References

[1] T. Loiseau, G. Férey, J. Mater. Chem. 6 (1996) 1073.
[2] G.Y. Yang, S.C. Sevov, J. Am. Chem. Soc. 121 (1999) 8389.
[3] D. Riou, G. Férey, Eur. J. Solid State Inorg. Chem. 31 (1994) 605.
[4] P. Feng, X. Bu, G.D. Stucky, Nature 388 (1997) 735.
[5] K.F. Hsu, S.L. Wang, Chem. Commun. (2000) 135.
[6] F. Bonhomme, S.G. Thoma, M.A. Rodriguez, T.M. Nenoff, Microporous Mesoporous Mater. 47 (2001) 185.
[7] S.H. Luo, Y.C. Jiang, S.L. Wang, H.M. Kao, K.H. Lii, Inorg. Chem. 40 (2001) 5381.
[8] C. Schott-Darie, H. Kessler, M. Soulard, V. Gramlich, E. Benazzi, in: J. Weitkamp, H.G. Karge, H. Pfeifer, W. Hölderich (Eds.), Zeolites and Related Microporous Materials, State of the Art 1994, Studies Surface Science and Catalysis, Vol. 84A, Elsevier, Amsterdam, 1994, p. 101.
[9] H. Kessler, J. Patarin, C. Schott-Darie, in: J.C. Jansen, M. Stöcker, H.G. Karge, J. Weitkamp (Eds.), Advanced Zeolite Science and Applications, Studies Surface Science and Catalysis, Vol. 85, Elsevier, Amsterdam, 1994, p. 75.
[10] A. Meden, R.W. Grosse-Kunstleve, C. Baerlocher, L.B. McCusker, Z. Kristallogr. 212 (1997) 801.
[11] A.M. Chippindale, A.R. Cowley, Zeolites 18 (1997) 176.
[12] A.M. Chippindale, A.D. Bond, A.R. Cowley, A.V. Powell, Chem. Mater. 9 (1997) 2830.
[13] F. Bonhomme, S.G. Thoma, T.M. Nenoff, J. Mater. Chem. 11 (2001) 2559.
[14] K.H. Lii, C.Y. Chen, Inorg. Chem. 39 (2000) 3374.
[15] C.T.S. Chio, E.V. Anokhina, C.S. Day, Y. Zhao, F. Taulelle, C. Huguenard, Z. Gan, A. Lachgar, Chem. Mater. 14 (2002) 4096.
[16] L. Josien, A. Simon, V. Gramlich, J. Patarin, Chem. Mater. 13 (2001) 1305.
[17] L. Josien, A. Simon-Masseron, V. Gramlich, J. Patarin, Chem. Eur. J. 8 (2002) 1614.
[18] L. Josien, A. Simon-Masseron, V. Gramlich, J. Patarin, L. Rouleau, Chem. Eur. J. 9 (2003) 856.
[19] G.M. Sheldrick, SHELXS-86, Program for the Solution of Crystal Structures, University of Göttingen, Germany, 1986.
[20] G.M. Sheldrick, SHELXL-93, Program for Crystal Structure Determination, University of Göttingen, Germany, 1993.
[21] P.B. Moore, Am. Mineral. 57 (1972) 397.
[22] R.C.L. Mooney-Slater, Acta Crystallogr. 20 (1966) 526.
[23] T. Loiseau, G. Férey, Eur. J. Solid State Inorg. Chem. 31 (1994) 575.
[24] L. Beitone, T. Loiseau, G. Férey, Acta Crystallogr. Sect. C 58 (2002) I103.
[25] A. Guesdon, Y. Monnin, B. Raveau, J. Solid State Chem. 172 (2003) 237.
[26] J.J. Pluth, J.V. Smith, J.M. Bennett, J.P. Cohen, Acta Crystallogr. Sect. C 40 (1984) 2008.
[27] H.E. King, L.A. Mundi, K.G. Strohmaier, R.C. Haushalter, J. Solid State Chem. 92 (1991) 1.
[28] A. Guesdon, M.M. Borel, A. Leclaire, A. Grandin, B. Raveau, Z. Anorg. Allg. Chem. 619 (1993) 1841.
[29] A. Leclaire, M.M. Borel, A. Grandin, B. Raveau, J. Solid State Chem. 108 (1993) 46.
[30] V. Soghomonian, L.A. Meyer, R.C. Haushalter, J. Zubieta, Inorg. Acta 275 (1998) 122.
[31] K.O. Kongshaug, H. Fjellvåg, K.P. Lillerud, Microporous Mesoporous Mater. 32 (1999) 17.
[32] K.O. Kongshaug, H. Fjellvåg, K.P. Lillerud, Microporous Mesoporous Mater. 40 (2000) 313.
[33] J.B. Parise, Inorg. Chem. 24 (1985) 4312.
[34] K.H. Lii, Y.F. Huang, Chem. Commun. (1997) 839.
[35] A.M. Chippindale, K.J. Peacock, A.R. Cowley, J. Solid State Chem. 145 (1999) 379.
[36] R.I. Walton, F. Millange, T. Loiseau, D. O'Hare, G. Férey, Angew. Chem. Int. Ed. 39 (2000) 4552.
[37] A.M. Chippindale, A.R. Cowley, J. Solid State Chem. 159 (2001) 59.
[38] A. Matijasic, V. Gramlich, J. Patarin, Solid State Sci. 3 (2001) 155.
[39] A. Matijasic, V. Gramlich, J. Patarin, J. Mater. Chem. 11 (2001) 2553.
[40] I.D. Brown, in: M. O'Keeffe, A. Navrotsky (Eds.), Struct. Bonding Cryst., Vol. 2, Academic Press, New York, 1981, p. 1 Chap. 14.
[41] A. Matijasic, J.L. Paillaud, J. Patarin, J. Mater. Chem. 10 (2000) 1345.